RELATIVE INSENSITIVITY TO INHOMOGENEITIES ON VERY HIGH ENERGY ELECTRON DOSE DISTRIBUTIONS

A. Lagzda*[1,2], R.M. Jones[1,2], D. Angal-Kalinin[2,3], J. Jones[2,3], A. Aitkenhead[4,1], K. Kirkby[4,1], R. McKay[4,1], M. van Herk[4],W. Farabolini[5], S. Zeeshan[5]
[1] University of Manchester, Manchester, United Kingdom
[2] Cockcroft Institute, Daresbury, United Kingdom, [3] ASTeC, Daresbury, United Kingdom
[4] The Christie NHS Trust, Manchester, United Kingdom, [5] CERN, Meyrin, Switzerland

Abstract

We investigated the effects of heterogeneous regions on dose deposition of very high-energy electrons (VHEE) using both Geant4 simulations and experiments performed at the CALIFES facility at CERN. Small air and acetal plastic (bone equivalent) cavities were embedded in a water phantom and irradiated with a 197 MeV electron beam. Experimentally determined transverse dose profiles were acquired using radiation sensitive EBT3 Gafchromic films embedded in the water phantom at various depths. EBT3 Gafchromic films were found to be a suitable dosimeter for relative dose dosimetry of VHEE beams. Simulated and measured results were found to be consistent with each other and the largest discrepancy was found to be no more than 5%. Dose profiles of VHEE beams were found to be relatively insensitive to embedded high and low density geometries.

INTRODUCTION

Recent advances in compact high-gradient (> 50 MV/m) accelerator technology [1–4] have revived interest in using very-high energy electrons (VHEE) in the 50 – 250 MeV energy range [5] for radiotherapy of deep-seated tumours, which are currently most commonly treated using multi-MV (MegaVolt) photon radiotherapy. Electrons produced by present day medical linear accelerators (linacs) have energies in the range of 5 – 25 MeV [6]. In this energy range electrons are well-suited to superficial tumour treatment, as a large fraction of the dose is deposited very close to the skin surface, followed by a sharp cut-off a few centimeters within the tissue. In this energy range electrons are of course not suitable for deep-seated tumour treatment.

VHEE beams are able to penetrate deeper. Moreover, recent simulation and experimental studies have highlighted various potential advantages of VHEE beams over conventional MV photon beams, such as higher dose reach in tissue, more conformal dose deposition, the potential for higher dose rate and a possibility for magnetic beam steering within the patient volume [7–11].

Furthermore, understanding the dosimetric properties of particle beams at various density region interfaces is essential in order to plan and deliver optimal radiotherapy treatments to patients. This is because discrepancies in high and low density regions in the irradiation volume, such as lung and bone, can significantly alter the delivered dose distribution. In particular, underestimation of the total irradiation required in a cancerous region during proton therapy, for example, may result in parts of a tumour failing to be irradiated due to a shift in the Bragg peak position and healthy tissue receiving a high dose [12]. In MV photon therapy a dose build-up is observed after low-density regions [13]. However, as our simulations reveal, VHEE beams are relatively insensitive to intervening inhomogeneities.

We studied the effects of high and low density regions embedded in water phantoms on VHEE beam dose profiles and the corresponding beam spread. In the following section Monte Carlo particle tracking simulations are performed to ascertain dose profiles in various media. These simulations are confirmed in the section thereafter, which consists of a description of experiments made at CERN and a discussion on the results. The concluding section consists of final remarks.

SIMULATIONS OF DOSE DEPOSITION

We used the Geant4 (GEometry ANd Tracking) particle tracking code to simulate the experimental set-up. Geant4 is an object-oriented Monte Carlo toolkit written in the C++ computer language, and is designed to simulation particle transport through matter [14–16].

In our studies with Geant4 for VHEE beams we have shown these beams are able penetrate depths well-aligned to deep-seated tumours. A typical example of this is displayed in the two-dimensional (2D) dose distribution maps in Fig. 1.

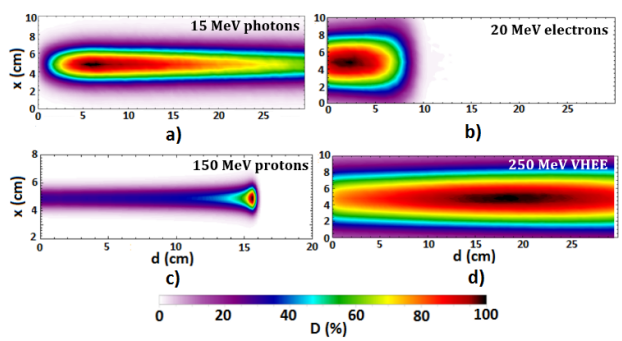

Figure 1: Central plane dose distribution of: (a) a photon beam at 15 MeV, (b) a 20 MeV electron beam, (c) a 150 MeV proton beam and (d) a 250 MeV electron beam. All beams are incident from the left and consist of an initial Gaussian charge distribution of 10^7 particles penetrating water.

* agnese.lagzda@postgrad.manchester.ac.uk

ISBN 978-3-95450-182-3

We also performed a series of experiments on a water phantom at the CALIFES (*Concept d'Accélérateur Linéaire pour Faisceau d'Electron Sonde*) facility in CERN. Prior to making these experiments we simulated the dose deposition in the phantom. For these simulations we used the following parameters: an electron beam with 10^7 particles normally incident upon a 30×30×30 cm^3 water phantom surrounded by 8 mm thick PMMA (Poly(methyl methacrylate)) walls. The dose scoring volume was comprised of $0.1 \times 0.1 \times 0.1$ mm^3 voxels. The secondary particle production cut-off threshold in Geant4 was set to 1 mm. Experimentally measured beam energy and spatial spread were included in the simulations. We compared these simulated dose distributions to experimental results in terms of longitudinal dose profiles and beam spread in water. Details of this experiment are given in the next section.

EXPERIMENTAL SETUP

We conducted a series of experimental measurements using the 197 MeV electron pencil beams (FWHM = 2 mm) at the CALIFES facility at CERN. The experiment was conducted using a set of EBT3 Gafchromic films submerged and irradiated at various depths in a cuboid water phantom (30×30×30 cm^3) with 8 mm thick PMMA walls. The EBT3 dosimetric film is composed of three layers: an active layer surrounded by two polyester bases. Exposing the film to ionizing radiation results in a production of a blue-coloured polymer in the active layer. This darkening of the film was measured from 16-bit images using an EPSON 10000XL flatbed scanner in terms of the film's optical density (OD) given by [17]

$$\mathrm{OD} = -\log_{10}\left(\frac{\mathrm{PV}}{2^{16}-1}\right), \qquad (1)$$

where PV refers to the red, green or blue scanned pixel values.

Dosimetric effects of heterogeneous regions were investigated by embedding a spherical air capsule (ρ = 1.225 kg/m^3, r = 2 cm) and an acetal plastic cuboid (ρ = 1.45 kg/m^3, d = 15 mm) in a water phantom.

The phantom was placed on a stage equipped with a remotely controlled transverse movement ≈40 cm away from a 0.5 mm thick aluminum exit window. Beam parameters of a typical irradiation run are tabulated in Table 1. The schematic of the irradiation set-ups are shown in Figure 2.

EBT3 Dose Response Calibration for VHEE beams

No extant data for EBT3 film response to VHEE beams was available. Therefore, in order to determine the relation between the OD and delivered dose, the EBT3 film was placed at a 3 cm depth in water and irradiated with various number of ≈ 50 pC charge pulses (see Table 2) with a repetition rate of 1.3 Hz.

The dose response of VHEE beams at a 3 cm depth in water was estimated using Monte Carlo simulations in Geant4.

Table 1: Main Beam Parameters of CALIFES

Beam parameter	Value
Energy	197 MeV
Energy spread	< 0.5 MeV
Bunch charge	0.05 nC
Train Length	50
Charge jitter	≈ 20 %
Repetition rate	1.3 Hz
Beam size (FWHM)	2.02 mm

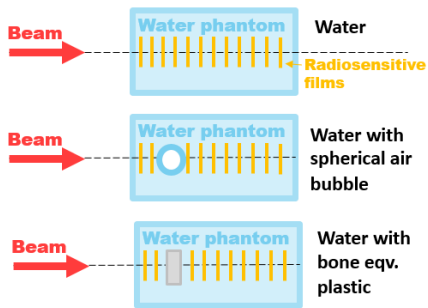

Figure 2: Schematic of irradiation set-ups.

The dose was simulated at this depth and was used as a reference frame for all measured dose profiles. The dose response D of the film was fitted to a power law of the following functional form:

$$\mathrm{D} = A \cdot B^{\mathrm{OD}} + C. \qquad (2)$$

where A, B and C are constants obtained from the fit and OD is the optical density of the material.

The quoted effective dose range by the manufacturers of the EBT3 films is up to 10 Gy. Beyond this point the red and the green channels were found to saturate. However, by analyzing the blue channel response, it was possible to successfully use EBT3 films for dose ranges up to 100 Gy.

COMPARISON OF EXPERIMENTAL RESULTS AND SIMULATIONS IN WATER

The dose maps of 197 MeV VHEE beams for various depths in water are shown in Fig. 3. Due to the relatively small beam width (FWHM = 2.02 mm at the water phantom surface), the beam diverges and the dose attenuates rapidly

Table 2: Charge Measurements During Film Calibration

No. of shots	Avg. charge (pC)	Total charge (nC)
10	47.5 ± 0.1	0.4752 ± 0.0004
31	46.7 ± 0.5	1.4490 ± 0.0149
40	46.7 ± 0.3	1.8678 ± 0.0124
80	45.2 ± 0.2	1.4490 ± 0.0234
120	43.7 ± 0.1	1.4490 ± 0.0139

in water. No distinguishable signal was detected in the film beyond a depth of 20 cm.

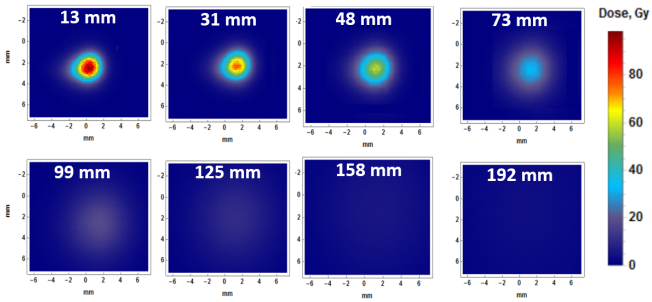

Figure 3: Transverse dose of VHEE beams at various depths.

Simulated dose profiles and beam spread curves of a 197 MeV VHEE beam in water were compared with experimental measurements at various depths and these are shown in Fig. 4 and 5. Differences between measured and simulated dose profiles and beam spread curves were <5%.

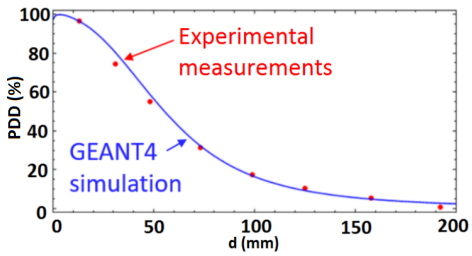

Figure 4: Experimental measurements (red markers) and simulated (blue line) on-axis dose Percentage Depth Dose (PDD) versus depth d.

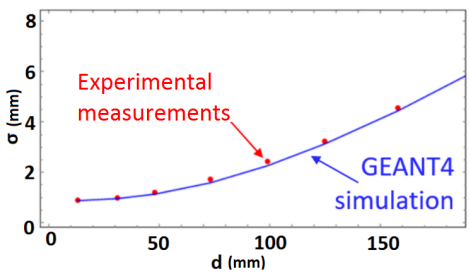

Figure 5: Experimental measurements (red markers) and simulated (blue line) transverse beam σ versus depth d.

DOSE DEPOSITION IN VARIOUS MEDIA

To determine the sensitivity to heterogeneous media we experimentally investigated the dose deposition in several media. We studied longitudinal dose profiles in a water phantom with and without inserts of various density materials. The results of these experiments are collated in Figs. 6 and 7. The points correspond to experimental measurements and the curves to a least square cubic spline fit to each data set. It is evident that the dose profile and the beam spread of these VHEE beams are relatively unaffected by the addition of both high density and low density intervening media.

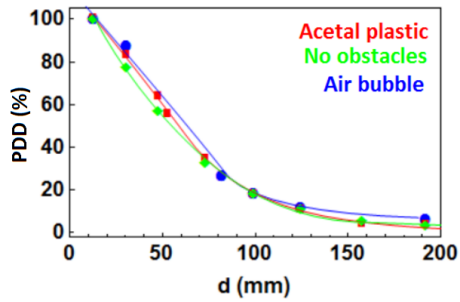

Figure 6: Percentage depth dose (PDD) curves for 197 MeV VHEE beams in water with air and acetal geometry positions highlighted on the plot.

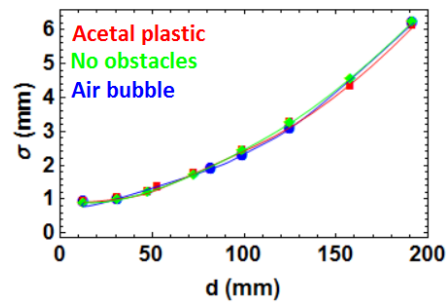

Figure 7: Transverse σ versus depth d of 197 MeV VHEE beams in homogeneous water and heterogeneous targets.

Finally we note that all experiments relied on the beam measurement set-up, and there are several sources of uncertainty. The main source of uncertainties in the measurements is the relatively low response of the blue channel below a dose of 20 Gy, as well as beam energy drift and charge jitter. The water phantom is immediately after a dipole bending magnet. Changes in beam energy over the irradiation time of ($\approx$ 1 min) resulted in an observed horizontal smear in several transverse dose maps (Fig. 3). No appreciable dose smearing was observed in vertical measurements.

FINAL REMARKS

The measured and simulated dose deposition of VHEE beams in water are consistent with each other. The observed dose profile and beam spread independence of the intervening media indicates that VHEE has the potential to be a reliable mode of radiotherapy for treating tumours in highly inhomogeneous and mobile regions such as lung.

ACKNOWLEDGEMENTS

The authors acknowledge support received from the Cockcroft Institute and ASTeC to help facilitate the water phantom setup and measurements. Colleagues at CERN provided invaluable assistance in facilitating the experiments at CALIFES.

REFERENCES

[1] E. Esarey, C. B. Schroeder, and W. P. Leemans, "Physics of laser-driven plasma-based electron accelerators," *Rev. Mod.*

Phys., vol. 81, pp. 1229–1285, Aug 2009.

[2] R.M. Jones, "Wakefield suppression in high gradient linacs for lepton linear colliders", *Phys. Rev. ST Accel. Beams 12*, pp.104801, 2009

[3] T. Higo, M. Akemoto, A. Enomoto, S. Fukuda, H. Hayano, N. Kudo, S. Matsumoto, T. Saeki, N. Terunuma, N. Toge, K. Watanabe, and T. Suehara, "High gradient study at kek on x-band accelerator structure for linear collider," in *Proceedings of the 2005 Particle Accelerator Conference*, pp. 1162–1164, May 2005.

[4] J. W. Wang, G. A. Loew, R. J. Loewen, R. D. Ruth, A. E. Vlieks, I. Wilson, and W. Wuensch, "SLAC/CERN high gradient tests of an X-band accelerating section," in *Particle Accelerator Conference, 1995., Proceedings of the 1995*, vol. 1, pp. 653–655 vol.1, May 1995.

[5] C.M. DesRosiers, "An evaluation of very high energy electron beams (up to 250 MeV) in radiation therapy", Purdue University, Ph.D. thesis, 2000.

[6] K. R. Hogstrom and P. R. Almond, "Review of electron beam therapy physics," *Physics in Medicine and Biology*, vol. 51, no. 13, p. R455, 2006.

[7] C. DesRosiers, V. Moskvin, A. F. Bielajew, and L. Papiez, "150-250 mev electron beams in radiation therapy," *Physics in Medicine and Biology*, vol. 45, no. 7, p. 1781, 2000.

[8] C. Yeboah and G. A. Sandison, "Optimized treatment planning for prostate cancer comparing impt, vheet and 15 mv imxt," *Physics in Medicine and Biology*, vol. 47, no. 13, p. 2247, 2002.

[9] C. DesRosiers, V. Moskvin, M. Cao, C. Joshi, and M. Langer, "Lung tumor treatment with very high energy electron beams of 150-250 mev as compared to conventional megavoltage photon beams," *International Journal of Radiation Oncology* Biology* Physics*, vol. 72, no. 1, p. S612, 2008.

[10] M. Bazalova-Carter, M. Liu, B. Palma, M. Dunning, D. McCormick, E. Hemsing, J. Nelson, K. Jobe, E. Colby, A. C. Koong, S. Tantawi, V. Dolgashev, P. G. Maxim, and B. W. Loo, "Comparison of film measurements and monte carlo simulations of dose delivered with very high-energy electron beams in a polystyrene phantom," *Medical Physics*, vol. 42, no. 4, 2015.

[11] M. Bazalova-Carter *et al.*, "Treatment planning for radiotherapy with very high-energy electron beams and comparison of vhee and vmat plans," *Medical Physics*, vol. 42, no. 5, 2015.

[12] H. Paganetti, "Range uncertainties in proton therapy and the role of monte carlo simulations," *Physics in Medicine and Biology*, vol. 57, no. 11, p. R99, 2012.

[13] R. O. Ottosson, A. Karlsson, and C. F. Behrens, "Pareto front analysis of 6 and 15 mv dynamic imrt for lung cancer using pencil beam, aaa and monte carlo," *Physics in Medicine and Biology*, vol. 55, no. 16, p. 4521, 2010.

[14] J. Allison *et al.*, "Recent developments in geant4," *Nuclear Instruments and Methods in Physics Research Section A: Accelerators, Spectrometers, Detectors and Associated Equipment*, vol. 835, pp. 186 – 225, 2016.

[15] J. Allison *et al.*, "Geant4 developments and applications," *IEEE Transactions on Nuclear Science*, vol. 53, pp. 270–278, Feb 2006.

[16] S. Agostinelli *et al.*, "Geant4—a simulation toolkit," *Nuclear Instruments and Methods in Physics Research Section A: Accelerators, Spectrometers, Detectors and Associated Equipment*, vol. 506, no. 3, pp. 250 – 303, 2003.

[17] R. Wendt III *et al.*, "Principal Component Analysis of EBT2 Radiochromic Film for Multichannel Film Dosimetry," *International Journal of Medical Physics, Clinical Engineering and Radiation Oncology*, vol. 3, no. 3, pp. 156, 2014.